Chemical Science

Accepted Manuscript

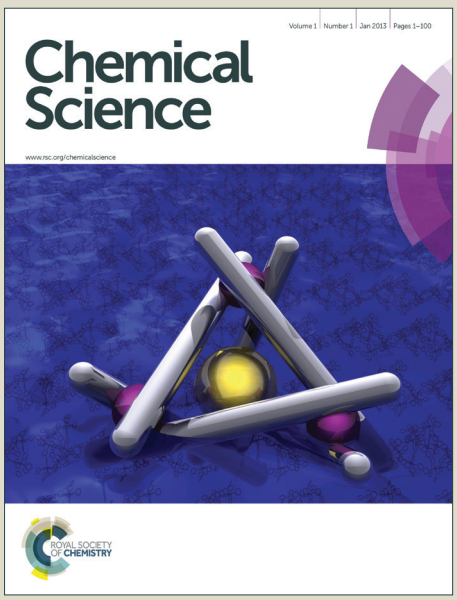

ROYAL SOCIETY OF CHEMISTRY

www.rsc.org/chemicalscience

Chemical Science

RSCPublishing

ARTICLE

On the Factors That Control the Reactivity of *meta*–Benzynes

Cite this: DOI: 10.1039/xoxxoooooox

Received ooth January 2012,
Accepted ooth January 2012

DOI: 10.1039/xoxxoooooox

www.rsc.org/

Jinshan Gao,[a] Bartłomiej J. Jankiewicz,[a] Jennifer Reece,[a] Huaming Sheng,[a] Christopher J. Cramer,[b] John J. Nash,*[a] Hilkka I. Kenttämaa*[a]

The reactivities of eleven 3,5–didehydropyridinium and six 2,4–didehydropyridinium cations toward cyclohexane were examined in the gas phase by using Fourier–transform ion cyclotron resonance (FT–ICR) mass spectrometry as well as high–level quantum chemical calculations. The results unequivocally demonstrate that the reactivity of *meta*–benzyne analogs can be "tuned" from more radical–like to less radical–like by changing the type and position of substituents. For example, σ–acceptor substituents at the 4–position and π–donor substituents at the 2–position in 3,5–didehydropyridinium cations partially decouple the biradical electrons, which results in lower energy transition states, and faster radical reactions. In contrast, σ–acceptors at the 2–position and π– donors at the 4–position in 3,5–didehydropyridinium cations cause stronger coupling between the biradical electrons, which results in lower radical reactivity. Three main factors are found to control the reactivity of these biradicals: (1) the energy required to distort the minimum energy dehydrocarbon atom separation to the separation of the transition state, (2) the S–T splitting at the separation of the transition state, and (3) the electron affinity at the separation of the transition state.

Introduction

Arynes[1,2] play a pivotal role in the biological activity of enediyne cytostatics,[3-5] combustion reactions,[6-8] heterogeneous catalysis,[9, 10] as well as nucleophilic addition and cycloaddition reactions in organic synthesis.[11-14] Hence, they have been the subject of many experimental and computational studies for the last few decades. In these studies, much effort has been dedicated to the elucidation of the thermochemical properties,[15-17] structures[18-28] and reactivity[29-38] of arynes with the benzene skeleton (benzynes) and to the improvement of the understanding of substituent effects[39-49] and ring heteroatoms[50-53] on the properties of these systems.

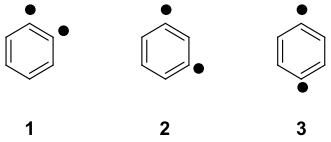

1 2 3

Fig. 1 Structures of *ortho*– (**1**), *meta*– (**2**), and *para*–benzyne (**3**).

The *ortho*–benzyne **1** (Chart 1) and its analogs are popular reagents in organic and organometallic synthesis procedures.[11-14, 54, 55] The existence of *ortho*–benzynes was firmly corroborated in 1942 and 1953 by Wittig[56] and Roberts,[57] respectively, although their existence as intermediates in various reactions had been hypothesized as early as 1870.[58] They have been thoroughly studied computationally and experimentally due to the relative ease with which they can be generated in solution, compared to the other benzynes. These studies have resulted in the measurement of the IR spectrum of *ortho*–benzyne isolated in low-temperature matrices,[59-64] NMR spectra of *ortho*–benzyne trapped in a hemicarcerand[65] and a microwave spectrum of *ortho*–benzyne in the gas phase.[66] The heat of formation of *ortho*–benzyne (106.6 kcal mol^{-1}) has been determined by threshold collision–activated dissociation (CAD) experiments[15] and its singlet–triplet (S–T) splitting (–37.5 kcal mol^{-1}; S–T splitting is defined as the energy difference between the lowest energy singlet state and the lowest energy triplet state) has been measured using negative ion photoelectron spectroscopy (NIPES).[17] The *ortho*–benzyne has a large S–T splitting[17] due to a strong through–space coupling between the radical sites. Hence, a large amount of energy is required to uncouple the biradical electrons, which is the reason for the nonradical–type reactivity observed for *ortho*–benzyne and its analogs.[29]

The *para*–benzyne **3**, was generated for the first time by Jones and Bergman by pyrolysis of *cis*–3–hexen–1,5–diyne and verified through isotope–labeling and product trapping experiments in 1972.[67] Although *para*–benzyne and its analogs have been studied ever since, the most significant interest in *para*–benzynes was piqued by the discovery in the 1990s of the naturally–occurring anticancer antibiotics (calicheamicins, esperamicins and dynemicins) that contain an enediyne group and whose bioactivity is associated with the in vivo formation of *para*–benzyne derivatives.[3, 4,68-71] These intermediates are formed in cycloaromatization reactions of enediyne derivatives, now referred to as Bergman cyclizations.[72-77] Unlike *ortho*–benzyne analogs, *para*–benzyne derivatives can undergo radical reactions. When interacting with DNA, they abstract a hydrogen atom from deoxyribose in both strands of double–stranded DNA, causing irreversible DNA cleavage (Figure 1). Unfortunately, the delayed high cytotoxicity of these antibiotics hinders their clinical use.[78]

Sander and co–workers have generated *para*–benzyne (**3**) in an argon matrix by flash photolysis and measured its infrared spectrum.[42] The *para*–benzyne has been measured to have a heat of formation of 137.3 kcal mol^{-1} and a S–T splitting of –3.8 kcal mol^{-1} by Wenthold et al.[15, 17] The magnitude of the S–T splitting has been proposed to be the main factor controlling the reactivity of *para*–benzynes and other related singlet biradicals by Chen et al.[79, 80] Since *para*–benzyne has a much smaller S–T splitting[17] than *ortho*–benzyne due to the weak interaction between the radical sites via through–bond coupling, *para*–benzyne and its analogs are expected to react exclusively via radical pathways.[79,80] However, the through–bond coupling significantly reduces their reaction rates compared to those of related monoradicals.[70, 81] The partial uncoupling of the two biradical electrons in the transition state increases its energy by some amount that has been presumed to be related to the magnitude of the S–T splitting.[79, 80]

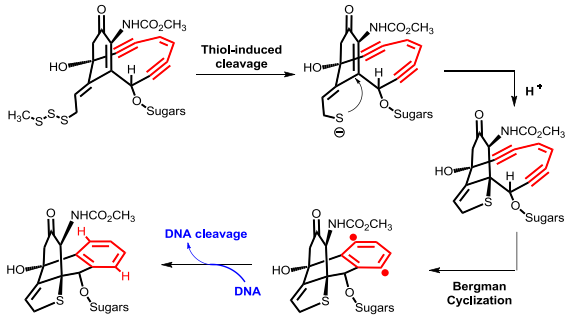

Fig. 2 Proposed mechanism of action for calicheamicin, an enediyne antitumor drug.

meta–Benzyne (**2**) and its derivatives have not received the same degree of attention that has been lavished upon the *ortho*– and *para*–benzynes and their analogs. In 1975, *meta*–benzyne was first generated by dehydrohalogenation of *exo*,*exo*–2,6–dibromo-bicyclo[3,1,0]–hex–2–ene by Washburn.[82] Since then, several methods, including pyrolysis, flash vacuum pyrolysis, and photolysis, have been developed to generate *meta*–benzyne and its analogs.[83-86] IR spectra of substituted *meta*–benzynes in low temperature matrices have been measured.[39,40,45,48,87,88] *meta*–Benzyne has been determined[15] to have a heat of formation of 122.0 kcal mol^{-1} and a S–T splitting of –21.0 kcal mol^{-1},[17] which is smaller than that of *ortho*–benzyne but larger than that of *para*–benzyne. The two radical sites in *meta*–benzyne interact not only via through–space overlap of the nonbonding orbitals but also via through–bond overlap with the intervening C–H bond.[89] Early trapping experiments in solution suggested that both bicyclic[82,90] and biradical[91,92] structures are possible for *meta*–benzyne. Recently, *meta*–benzyne was conclusively shown to have a biradical rather than a bicyclic structure via computational studies and measurement of an IR spectrum for matrix isolated *meta*–benzyne.[40,45,48,85,86]

Given that *meta*–benzyne analogs have strong coupling between the radical sites, which reduces their radical reactivity, they might make a more selective "warhead" for antitumor agents than *para*–benzyne analogs. Therefore, an improved understanding of the factors that control the reactivity of *meta*–benzyne and its analogs could be beneficial for the rational design of synthetic DNA cleaving agents. Unfortunately, solution reactivity studies of the benzynes, with the exception of *ortho*–benzyne and its analogs, are a challenge due to their high reactivities and the difficulty in generating them cleanly in condensed phases.[1, 2] Many of the problems associated with studies of reactive intermediates in solution become irrelevant in the gas phase. Indeed, many exceedingly reactive ionic species have been investigated in great detail by mass spectrometric techniques.[32, 93] These techniques can be extended to reactive neutral molecules via ions that contain the reactive group of interest and a chemically inert charged group for mass spectrometric manipulation ("distonic ion approach").[68] One benefit associated with such experiments is that intrinsic (solvent free) properties can be explored, which provides information that is crucial for the understanding of reactivity in any environment.

Compared to the parent *meta*–benzyne, 1,3–didehydrobenzene, related heteroaromatic *meta*–benzyne analogs, such as pyridynes, are much less studied. Protonated pyridynes have been used as surrogates to explore the reactivity of a few *meta*–benzyne analogs in the gas phase.[30-34] However, they also are interesting because their reactivity can be influenced by not just the S–T splitting but also by their polarity (protonated vs. unprotonated biradicals). As expected, based on their large S–T splittings, most of these

positively charged *meta*–benzyne analogs were found to react as electrophiles rather than as radicals.[32] Further, just like for polar monoradicals,[93] the (calculated) vertical electron affinity (EA) of their radical site(s) was found to be the main factor for controlling their reactivity by influencing the polarization of the transition state. Vertical electron affinity (EA) is defined here as the energy released upon abstraction of an electron by the radical site(s) with no geometry change (consideration of the adiabatic values leads to the same conclusions). The greater the EA, the more polar the transition state, the lower its energy and the faster the reaction. This can be rationalized by employing the ionic avoided curve crossing model developed by Anderson et al. for monoradicals.[70]

Later, the dehydrocarbon atom separation (DAS) was found to be another important reactivity controlling factor for *meta*–benzyne analogs[36] when it was discovered that some *meta*–benzyne analogs with unusually large DAS actually underwent radical reactions in spite of their large S–T splittings. This reactivity controlling parameter is best understood by considering the zwitterionic resonance structure of *meta*–benzyne proposed earlier by Cramer and Johnson (Figure 2) to explain computational results on the structures of substituted *meta*–benzynes.[47,94] These studies have shown that different types of substituents on different positions in *meta*–benzyne may stabilize or destabilize the bicyclic zwitterionic resonance structure (Figure 2), resulting in an increase or decrease in DAS. However, the reasons why DAS influences the reactivity of *meta*–benzyne analogs were still unclear.[36]

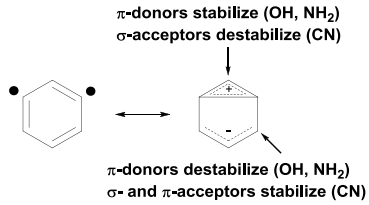

Fig. 3 Substituent effects on the stability of a bicyclic zwitterionic resonance structure of *meta*–benzyne.

Here, results obtained in a kinetic reactivity study on seventeen positively charged *meta*–benzyne analogs (Chart 2) toward a hydrogen atom donor, cyclohexane, are discussed. Cyclohexane was chosen as the substrate since the abstraction of two hydrogen atoms from this reagent usually occurs via a radical mechanism.[93, 95] The biradicals studied include eleven 3,5–didehydropyridinium cations (4–cyano– (**4**), 4–fluoro– (**5**), 4–chloro– (**6**), 4–amino– (**7**), and 4–hydroxy–3,5–didehydropyridinium cations (**8**), 3,5–didehydropyridinium cation (**9**), and 2–cyano– (**10**), 2–fluoro– (**11**), 2–chloro– (**12**), 2–amino– (**13**), and 2–hydroxy–3,5–didehydropyridinium cations (**14**)), as well as six 2,4–didehydropyridinium cations (2,4–didehydropyridinium cation (**15**) and 3–hydroxy– (**16**), 3–fluoro– (**17**), 3–cyano– (**18**), 5–hydroxy– (**19**), and 5–cyano–2,4–didehydropyridinium cations (**20**)). The experimental and computational results provide insights into substituent effects on the chemical properties of these *meta*–benzyne analogs.

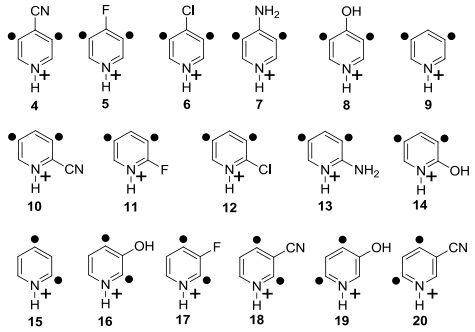

Fig. 4 Structures of the didehydropyridinium cations studied.

Experimental Section

Radical precursors and FT-ICR

Cyclohexane was purchased from Sigma–Aldrich and used as received. The biradical precursors (4–cyano–, 4–fluoro–, 4–chloro–, 4–amino–, 4–hydroxy–, 2–cyano–, and 2–fluoro–3,5–diiodopyridines for **4**–**8**, **10**, and **11**, respectively, and 3–cyano–, 5–hydroxy–, and 5–cyano–2,4–diiodopyridines for **18**–**20**, respectively) were synthesized according to literature procedures.[96-100] The 4–cyano–, 4–fluoro–, 2–cyano–, and 2–fluoro–3,5–diiodopyridines and the 3–cyano– and 5–cyano–2,4–diiodopyridines were synthesized here for the first time. The characterization of these compounds by ^{1}H, ^{13}C NMR, HRMS (high resolution mass spectrometry) and IR is discussed in detail in the Supporting Information. Two precursors (2–chloro– and 2–amino–3,5–diiodopyridine for biradicals **12** and **13**, respectively) were purchased from Alfa Aesar. The precursor for biradical **14**, 2–hydroxy–3–iodo–5–nitropyridine, was purchased from Sigma–Aldrich. Three precursors (3,5-, 2,4-, and 3-hydroxy-2,4-diiodopyridine for biradicals **9**, **15**, and **16**, respectively) were purchased from SynChem OHG. The precursor for biradical **17**, 3-fluoro-2,4-diiodopyridine, was purchased from Frontier Scientific.

All experiments were carried out in a Finnigan FTMS 2001 dual–cell FT–ICR mass spectrometer equipped with an Odyssey data station and a SWIFT (Stored Waveform Inverse Fourier Transform) cell controller as described previously, with details given in *Supporting Information*.[93] Briefly, the biradical precursors were ionized by chemical ionization in the source cell of the dual–cell FT-ICR mass spectrometer to generate protonated biradical precursors. These ions were transferred into the analyzer cell by changing the voltages of the trapping plates. The radical sites were generated by sustained off–resonance irradiated collision–activated dissociation.[101] The charged biradicals of interest were isolated and allowed to react with cyclohexane. The efficiency of each reaction (i.e., the fraction of collisions that leads to reaction) is given by k_{exp}/k_{coll}, wherein the k_{exp} represents the experimental reaction rate constant while k_{coll} represents the theoretical collision rate constant calculated using a parameterized trajectory theory.[102] The relative abundances of the primary products are reported as branching ratios, which are given as the ratio of the abundance of a primary product ion to the sum of the abundance of all primary products.

Computational methods

Geometries for all species were computed by using density functional theory (DFT) with the correlation–consistent polarized valence–triple–ζ (cc–pVTZ[103]) basis set. These DFT calculations use the gradient–corrected exchange functional of Becke,[104] which is combined with the gradient-corrected correlation functional of Lee, Yang and Parr[105] (B3LYP). B3LYP, like many early generation functionals, is known to do poorly for the calculation of medium-range correlation effects that strongly influence non–bonded interaction energies. However, for the analyses herein, such interactions are expected to be unimportant. All DFT geometries were verified to be local minima by computation of analytic vibrational frequencies, and these (unscaled) frequencies were used to compute zero–point vibrational energies (ZPVE) and 298 K thermal contributions ($H_{298} - E_0$) for all species. DFT calculations for triplet states of the biradicals employed an unrestricted formalism. Total spin expectation values for Slater determinants formed from the optimized Kohn–Sham orbitals did not exceed 2.03. For singlet biradicals, the DFT "wave function" was allowed to break spin symmetry by using an unrestricted formalism.[51,106-109] Total spin expectation values for Slater determinants formed from the optimized Kohn–Sham orbitals in these cases ranged widely between 0.0 and 1.0. Geometry optimization using the unrestricted formalism has been shown to give more accurate geometries for a number of relevant aromatic biradicals.[17, 26, 27, 47, 51, 52, 74, 80, 106-112]

Coupled–cluster calculations for single–configuration, restricted Hartree–Fock, reference wave functions were performed for all species. These calculations were of the single–point variety and included all single and double excitations and a perturbative estimate for triple excitations (i.e., RHF–UCCSD(T)/cc–pVTZ//B3LYP/cc–pVTZ). For the lowest energy triplet and singlet states of the biradicals, the T1 diagnostic did not exceed 0.018 except for the singlet states of **19** and **20** (0.027 and 0.030, respectively). For the zwitterionic doublet states (see below), the T1 diagnostic ranged from 0.013 to 0.038.

Molecular geometries for biradicals **4**–**20** and methane, as well as the hydrogen–atom abstraction transition states for each of the biradicals with methane, were also optimized at the MPW1K level of theory[113,114] by using the 6–31+G(d,p) basis set.[115-119] The MPW1K functional is a modification of the Perdew–Wang gradient–corrected exchange functional, with one parameter optimized to give the best fit to kinetic data for forty radical reactions.[113] All MPW1K geometries were verified to be local minima (or transition states) by computation of analytic vibrational frequencies, and these (unscaled) frequencies were used to compute zero–point vibrational energies (ZPVE) and 298 K thermal contributions ($H_{298} - E_0$) for all species. "Activation enthalpies" for the biradicals were computed as the difference in enthalpy between the transition state and the separated reactants (i.e., biradical and methane). MPW1K calculations for the biradicals and the transition states employed an unrestricted formalism.

For the singlet state of each biradical, the geometry was optimized (B3LYP/cc–pVTZ) at varying dehydrocarbon atom separations (ranging from 1.30 Å to 2.30 Å) by holding the dehydrocarbon atom separation constant and optimizing all other geometric parameters. Single–point calculations (RHF–UCCSD(T)/cc–pVTZ) were then performed for each (partially) optimized structure in order to determine the relative energies (i.e., with respect to the minimum energy structure) as a function of dehydrocarbon atom separation. The potential energy surfaces obtained at the RHF–UCCSD(T)/cc–pVTZ//UB3LYP/cc–pVTZ level of theory are quite different from those obtained at the UB3LYP/cc–pVTZ//UB3LYP/cc–pVTZ level (see Supporting Information). The poor performance of hybrid DFT methods (such as B3LYP), and much better performance of coupled–cluster methods, for the calculation of such potential energy surfaces has been noted previously for *meta*–benzyne.[120]

In order to compute vertical electron affinities for the biradicals at a dehydrocarbon atom separation of 2.30 Å, single–point calculations (RHF–UCCSD(T)/cc–pVTZ) using the B3LYP/cc–pVTZ partially optimized geometries were also carried out for the states that are produced when a single electron is added to one of the nonbonding σ orbitals of the biradical (singlet ground state).[121] Thus, these calculations were carried out for (zwitterionic) *doublet* states.[122] The vertical electron affinities of the biradicals were computed as [E_0(biradical; singlet state)] – [E_0(biradical + electron; doublet state)]. Note that because these are vertical electron affinities, zero–point vibrational energies (ZPVEs) and 298 K thermal contributions to the enthalpy are not included.

Quantum chemical calculations were carried out with the Gaussian 03[123] and Molpro[124] electronic structure program suites.

Results and Discussion

Experimental disquisition

The reactions and their efficiencies, as well as the branching ratios for the primary products, are given in Table 1 for reactions of biradicals **4**–**20** with cyclohexane. The table also shows calculated S–T splittings (ΔE_{S-T}), electron affinities at a dehydrocarbon atom separation of 2.30 Å ($EA_{2.30}$), dehydrocarbon atom separations for the minimum energy ground-state geometries, and the energy needed for each biradical to achieve the dehydrocarbon atom separation of 2.30 Å characteristic of their transition states for hydrogen atom abstraction ($\Delta E_{2.30}$; discussed in detail below). Biradicals **4**–**14** with the 3,5–didehydropyridinium cation structure will be discussed first.

As mentioned above, Chen and co–workers have suggested that the magnitude of the S–T splitting influences the reactivity of *para*–benzyne and its analogs.[79,80] Since the S–T splittings for the *meta*–benzyne analogs studied here are much larger (–16.6 to –36.0 kcal mol^{-1}) than those of *para*–benzyne[15,17] and its analogs (all ca. 4 kcal mol^{-1}), it has been suggested that they should not show radical reactivity.[79] However, some *meta*–benzyne analogs with large DASs were later shown to undergo radical reactions.[36] This finding was confirmed in the present study, as discussed below.

Three of the eleven 3,5–didehydropyridinium cations (**6**–**8**) were found to be unreactive toward cyclohexane, as expected based on their relatively large S–T splittings (ΔE_{S-T}: –27.9 to –32.8 kcal mol^{-1}; Table 1). However, the other eight biradicals with somewhat smaller but still substantial S–T splittings (ΔE_{S-T}: –16.6 to –26.8 kcal mol^{-1}; Table 1) did react with cyclohexane. The predominant reaction is abstraction of two hydrogen atoms, presumably via a radical mechanism (evidence in support of this statement is provided below). Although the biradicals with the largest S–T splittings are unreactive, suggesting that the reactivity is predominantly controlled by the magnitude of ΔE_{S-T}, the reactivity of the reactive biradicals does not correlate with the magnitude of their S–T splitting. For example, based on the S–T splitting, 4–cyano–3,5–didehydropyridinium cation (**4**; ΔE_{S-T}: –22.1 kcal mol^{-1}) should show lower radical reactivity than **9** (ΔE_{S-T}: –21.7 kcal mol^{-1}) and **11**–**14** (ΔE_{S-T}: –18.2, –20.0, –16.7 and –16.6 kcal mol^{-1}, respectively; Table 1). However, the experimental results show that **4** reacts with cyclohexane (by abstraction of two hydrogen atoms) much faster than any of these molecules (Eff. = 22%, 0.1%, 4%, 0.2%, 1% and 4% for **4**, **9** and **11**–**14**, respectively; Table 1). Moreover, 4–fluoro–3,5–didehydropyridinium cation (**5**), 2–fluoro–3,5–didehydropyridinium cation (**11**) and 2–hydroxy–3,5–didehydropyridinium cation (**14**) reacted with identical efficiencies (4%; Table 1) although they have very different S–T splittings (ΔE_{S-T}: –26.8, –18.2 and –16.6 kcal mol^{-1} for **5**, **11** and **14**, respectively; Table 1). Clearly, the S–T splitting is not the only factor controlling the reactivity of the *meta*–benzyne analogs, and additional reactivity controlling factors need to be considered.

As mentioned above, the electron affinity (EA) of the radical site(s) has been shown to be the main factor controlling the reactivity of polar monoradicals and some *meta*–benzynes.[36,70,93,125] Before discussing this issue further, the geometries of *meta*–benzynes need to be considered since the values of their EAs are very sensitive to their geometries. For all seventeen biradicals studied here, the minimum energy geometry of the (ground) singlet state is calculated (B3LYP/cc–pVTZ//B3LYP/cc–pVTZ) to be bicyclic (DAS: 1.43–1.57 Å; Table1). MPW1K/6–31+G(d,p) //MPW1K/6–31+G(d,p) calculations for the transition states for hydrogen atom abstraction from methane (as a model for cyclohexane) show (Fig. 5) that the dehydrocarbon atom separation (DAS) in the transition state is nearly the same (from 2.267 Å to 2.304 Å)[126] for all of the *meta*–benzyne analogs studied here (note that we will approximate the DASs for the transition states as 2.30 Å in order to simplify the subsequent analysis and discussion). This DAS is very different from the DASs for the minimum energy geometries. More importantly, calculated EAs for the minimum energy bicyclic structures are substantially lower (by several eV) than calculated EAs for "open" (e.g., large DAS, such as 2.30 Å), non–bicyclic structures resembling the transition state geometry. We believe that the EA at the transition state geometry for a *meta*–benzyne is likely to be a much more important reactivity controlling factor than the EA at the minimum energy (ground state) geometry; thus, we focus the following discussion on the calculated EAs at a DAS of 2.30 Å ($EA_{2.30}$).

The different reaction efficiencies of 2–hydroxyl–3,5–didehydropyridinium cation (**14**) and 2–amino–3,5–didehydropyridinium cation (**13**) (Eff. = 4% and 1%, respectively; Table 1) with similar

S–T splittings (ΔE_{S-T}: –16.7 and –16.6 kcal mol^{-1} for **13** and **14**, respectively; Table 1) are likely due to the fact that **14** has a greater EA at the transition state geometry than **13** ($EA_{2.30}$: 5.99 and 6.42 eV for **13** and **14**, respectively; Table 1). However, similar considerations do not explain why 4–cyano–3,5–didehydropyridinium cation (**4**) shows greater reactivity than 2-cyano-3,5-didehydropyridinium cation (**10**) (Eff, = 22% and 0.1%, respectively; Table 1) since they have similar $EA_{2.30}$ and S–T splittings. Hence, additional reactivity controlling factors have to be considered.

Table 1. Reaction Efficiencies[a] and Product Branching Ratios[b] for Reactions of Biradicals **4**–**20** With Cyclohexane, and Calculated S–T Splittings (ΔE_{S-T}),[c] Electron Affinities at 2.30 Å ($EA_{2.30}$),[c,d] Dehydrocarbon Atom Separations (DAS)[d,e] and Relative Energies at DAS of 2.30 Å ($\Delta E_{2.30}$)[c,d].

	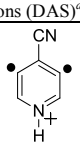 **4**	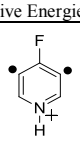 **5**	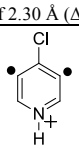 **6**	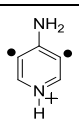 **7**	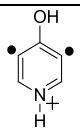 **8**	 **9**
ΔE_{S-T}, kcal mol^{-1}	-22.1	-26.8	-27.9	-32.8	-30.8	-21.7
$EA_{2.30}$, eV	6.97	6.82	6.63	5.93	6.42	6.35
DAS, Å	1.52	1.55	1.51	1.48	1.51	1.52
$\Delta E_{2.30}$, kcal mol^{-1}	5.0	6.3	9.7	11.9	9.7	6.3
	2 × H abs 90% H^- abs 10% Eff. = 22%	2 × H abs 68% Add. - HF 32% Eff. = 4%	No reaction	No reaction	No reaction	2 × H abs 100% Eff. = 0.1%
	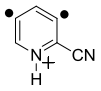 **10**	 **11**	 **12**	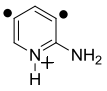 **13**	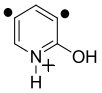 **14**	
ΔE_{S-T}, kcal mol^{-1}	-23.0	-18.2	-20.0	-16.7	-16.6	
$EA_{2.30}$, eV	6.97	6.71	6.59	5.99	6.42	
DAS, Å	1.50	1.54	1.53	1.56	1.57	
$\Delta E_{2.30}$, kcal mol^{-1}	8.5	4.6	6.0	3.7	3.6	
	2 × H abs 100% Eff. = 0.1%	2 × H abs 82% Add. - HF 18% Eff. = 4%	2 × H abs 100% Eff. = 0.2%	2 × H abs 100% Eff. = 1%	2 × H abs 100% Eff. = 4%	
	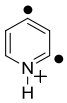 **15**	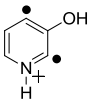 **16**	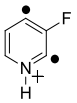 **17**	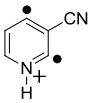 **18**	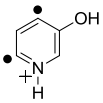 **19**	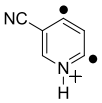 **20**
ΔE_{S-T}, kcal mol^{-1}	-24.4	-36.0	-31.3	-24.9	-20.0	-25.6
$EA_{2.30}$, eV	6.57	6.64	7.03	7.21	6.75	7.20
DAS, Å	1.45	1.43	1.46	1.44	1.46	1.43
$\Delta E_{2.30}$, kcal mol^{-1}	6.2	14.3	9.5	5.4	5.6	8.2
	2 x H abs 100% Eff. = 0.03%	No reaction	No reaction	2 x H abs 97% C_3H_6 abs 3% Eff. = 3%	2 x H abs 100% Eff. = 0.3%	No reaction

[a] Reaction efficiency (% of collisions leading to reaction) = kreaction/kcollision × 100; precision +10%; accuracy +50%. [b] abs = abstraction, Add. = addition. [c] Calculated at the RHF–UCCSD(T)/cc–pVTZ//B3LYP/cc–pVTZ level of theory. [d] For the (ground) singlet states. [e] B3LYP/cc–pVTZ optimized geometries.

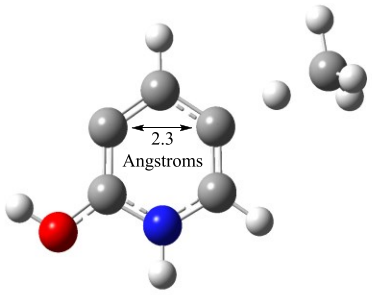

Fig. 5 Transition state for hydrogen atom abstraction from methane by **14** calculated at the MPW1K/6–31+G(d,p)//MPW1K/6–31+G(d,p) level of theory.

As mentioned above, the dehydrocarbon atom separation (DAS) has been suggested to be an important reactivity controlling factor for *meta*–benzyne analogs because radical reactions were observed for some *meta*–benzyne analogs with large DASs.[36] However, **4** and **10** (with similar S–T splittings and $EA_{2.30}$; described above) have almost identical DAS (Table 1); hence, their very different reactivities cannot be rationalized based on this parameter. In order to better understand DAS as a reactivity controlling parameter, potential energy surfaces for varying DAS (i.e., DAS was held constant and all other geometric parameters were optimized) were calculated for the singlet (ground) states of biradicals **4**–**14**. The calculated potential energy surfaces are all very flat (Fig. 6 and 7). These potential energy surfaces show that (1) the DAS of the minimum energy structures are similar (ca. 1.5 Å (bicyclic structures)) with the exception of **13** and **14** (ca. 2.0 Å) and (2) very little energy is required to increase or decrease the DAS within 1.4–2.1 Å. A closer examination of the calculated potential energy surfaces for **4**–**14** reveals that the energy required for each biradical to "distort" from the minimum energy geometry to the DAS in the transition state (ca. 2.30 Å; see above) varies markedly (Fig. 6 and 7). These "distortion energies"[68] ($\Delta E_{2.30}$) are listed in Table 1. It is noteworthy that biradicals **13** and **14** have very small values for $\Delta E_{2.30}$ (3.7 and 3.6 kcal mol^{-1}, respectively), presumably because the DAS for the minimum energy structures (ca. 2.0 Å; Fig. 7) are relatively close to the DAS in the transition state (2.30 Å). However, biradicals with similar or identical DAS for the minimum energy structures still can have very different $\Delta E_{2.30}$ values. In particular, 4–cyano–3,5–didehydropyridinium cation (**4**) and 2–cyano–3,5–didehydropyridinium cation (**10**) (with the same $EA_{2.30}$ (6.97 eV) and almost identical S–T splittings (–22.1 and –23.0 kcal mol^{-1}, respectively) and DAS (1.52 and 1.50 Å, respectively)) have quite different $\Delta E_{2.30}$ (8.5 and 5.0 kcal mol^{-1} for **10** and **4**, respectively; Table 1). Finally, this reactivity controlling parameter explains why **4** reacts with cyclohexane significantly faster than **10** (Eff.: **4**: 22%; **10**: 0.1%; Table 1). However, rationalization of the reaction efficiencies between any two of the other biradicals is not as straightforward because the values of at least two of the reactivity controlling parameters, ΔE_{S-T}, DAS, $EA_{2.30}$ and $\Delta E_{2.30}$, differ. The influence of these four reactivity controlling parameters on the reactivity of the biradicals is considered below.

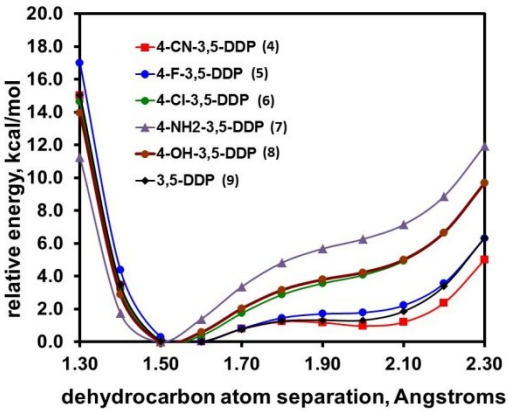

Fig. 6. Relative energy versus dehydrocarbon atom separation (DAS) for **4**–**9** (DDP = didehydropyridinium cation) calculated at the RHF–UCCSD(T)/cc–pVTZ//B3LYP/cc–pVTZ level of theory.

Based on the computed values of $\Delta E_{S\text{-}T}$, $EA_{2.30}$, DAS and $\Delta E_{2.30}$ for **4**–**14** given in Table 1, it is clear that the type and position of substituents have a significant effect on $\Delta E_{S\text{-}T}$ (–16.6 to –32.8 kcal mol^{-1}), $\Delta E_{2.30}$ (3.6–11.9 kcal/mol) and $EA_{2.30}$ (5.93–6.97 eV), but only a small effect on DAS for **4**–**12** (1.48–1.57 Å). Some of these differences can be rationalized qualitatively by considering the zwitterionic resonance structure of *meta*–benzyne (Fig. 3) discussed above.[9] For example, substituting 3,5–didehydropyridinium cation (**9**) at the 2–position with an OH group (to form **14**) or an NH_2 group (to form **13**) (Scheme 1) destabilizes the allyl anion part of the molecule due to an unfavorable π,π–interaction between the lone pair electrons on the oxygen or nitrogen atom and the allyl anion π–system, which results in relatively large DASs (i.e., at the RHF–UCCSD(T)/cc–pVTZ//B3LYP/cc–pVTZ level of theory; Fig. 7) for the minimum energy structures (and small $\Delta E_{2.30}$) for biradicals **13** and **14**. On the other hand, chlorine and fluorine substituents are less powerful π–donors than either OH or NH_2 groups. Both 2–chloro–3,5–didehydropyridinium cation (**12**) and 2–fluoro-3,5–didehydropyridinium cation (**11**) have smaller DASs (and, consequently, larger $\Delta E_{2.30}$ than either **13** or **14** (Fig. 7). In spite of containing a substituent that is not as good a π–donor as those in **13** and **14**, and a larger S–T splitting, **11** reacts with cyclohexane (Table 1) much faster than **13**, and at the same efficiency as **14**, which is most likely due to its much higher $EA_{2.30}$.

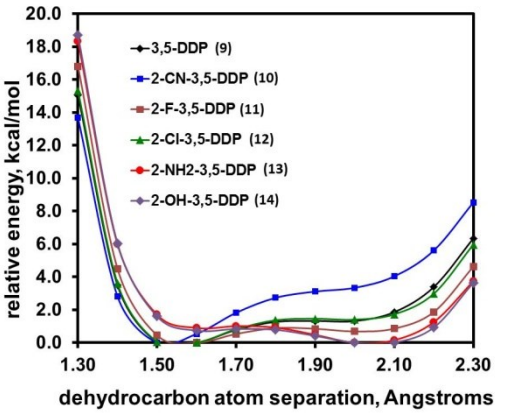

Fig. 7 Relative energy versus dehydrocarbon atom separation (DAS) for **9**–**14** (DDP = didehydropyridinium cation) calculated at the RHF–UCCSD(T)/cc–pVTZ//B3LYP/cc–pVTZ level of theory.

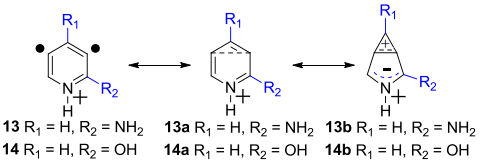

Scheme 1. Resonance Structures of **13** and **14**.

Substituting **9** at the 2–position with a CN group (**10**) (Scheme 1) should stabilize the allyl anion part of the zwitterionic resonance structure due to the strong electron withdrawing ability of the CN–substituent (a σ–acceptor group). Indeed, biradical **10** is calculated to have a similar DAS (Fig. 7), but a larger $\Delta E_{2.30}$ (8.5 kcal/mol; Table 1**)** and a slightly greater $\Delta E_{S\text{-}T}$ (–23.0 kcal mol^{-1}; Table 1) than **9**. Hence, biradical **10** should react slower with cyclohexane than biradical **9**. However, **10** has an $EA_{2.30}$ of 6.97 eV, which is much greater than that of **9** (6.35 eV; Table 1). Taking all of the reactivity controlling factors into consideration, and especially the large difference in $EA_{2.30}$, it is perhaps not surprising that biradical **10** reacts at the same rate as **9** with cyclohexane (Table1). This comparison, as well as the one discussed above, highlight the need to consider differences in electron affinity when evaluating the reactivity of *meta*–benzyne analogs.

Substituting **9** at the 4–position with a π–donor group (Scheme 1), such as NH_2 (**7**) or OH (**8**), should stabilize the cyclopropenium cation moiety (resonance structures **7a** and **8a**; Scheme 2) via delocalization of the charge to the oxygen or nitrogen atom to form the ionic resonance structures **7b** and **8b**. This stabilization is expected to produce a small DAS at the minimum energy geometry, and, consequently a relatively large $\Delta E_{2.30}$**.** Indeed, 4–amino–3,5–didehydropyridinium cation (**7**) and 4–hydroxy–3,5–didehydropyridinium cation (**8**) both have a large $\Delta E_{2.30}$ (11.9 and 9.7 kcal mol^{-1}**,** respectively; Table 1). This, coupled with the relatively large S–T splittings for these two biradicals (**7**: –32.8 kcal mol^{-1}; **8**: –30.8 kcal mol^{-1}) and their relatively low electron affinities (**7**: 5.93 eV; **8**: 6.42 eV; Table 1), explain why neither biradical reacts with cyclohexane.

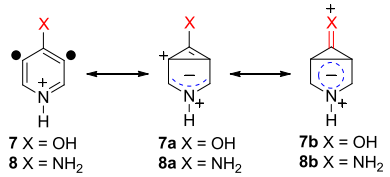

Scheme 2. Resonance Structures of **7** and **8**.

Based on the above results, $\Delta E_{S\text{-}T}$, $\Delta E_{2.30}$ and $EA_{2.30}$ are important reactivity controlling factors for the 3,5–didehydropyridinium cations **4**–**14**. In order to test the generality of this finding, a series of substituted 2,4–didehydropyridinium cations (**15**–**20**) was also examined. The calculated potential energy surfaces for the (ground) singlet states of **15**–**20** (Fig. 8) are quite flat, although perhaps not quite as flat as those for the 3,5–didehydropyridinium cations (Fig. 6 and 7). The reaction efficiencies of hydrogen atom abstraction from cyclohexane (Table 1) by the 2,4–didehydropyridinum cations also appear to depend on the aforementioned reactivity controlling factors. For example, despite their relatively high $EA_{2.30}$, the 3–hydroxy–, 3–fluoro–, and 5–cyano–2,4–didehydropyridinium cations (**16**, **17** and **20**) do not react with cyclohexane due to their relatively large S–T splittings and $\Delta E_{2.30}$ (Table 1)**.** An extreme example of the importance of $EA_{2.30}$ is provided by **15** and **18**, which have similar S–T splittings (–24.4 and –24.9 kcal mol^{-1}, respectively) and similar $\Delta E_{2.30}$ (6.2 and 5.4 kcal mol^{-1}, respectively), but very different $EA_{2.30}$ (6.57 and 7.21 eV, respectively; Table 1). In this case, **18** is two orders of magnitude more reactive than **15** (3% and 0.03%, respectively; Table 1). A comparison of the reactivity of **18** and **19** yields a similar conclusion. For these two biradicals, $\Delta E_{2.30}$ is nearly the same (5.4 and 5.6 kcal mol^{-1}, respectively), and $\Delta E_{S\text{-}T}$ is smaller for **19** than for **18** (–20.0 and –24.9 kcal mol^{-1}, respectively; Table 1), which should make **19** more reactive than **18**. However, $EA_{2.30}$ for **18** is much larger than that for **19** (7.21 and 6.75 eV, respectively) and counterbalances the difference in $\Delta E_{S\text{-}T}$ making **18** an order of magnitude more reactive than **19** (3% and 0.3%, respectively; Table 1).

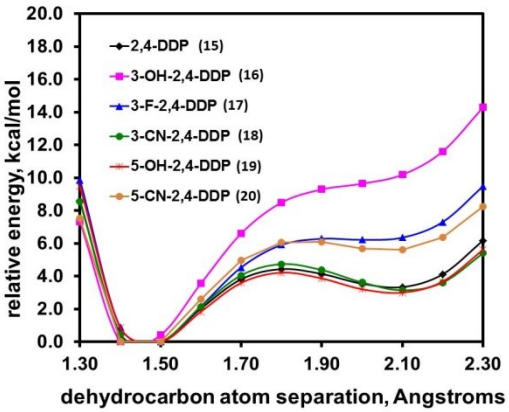

Fig. 8 Relative energy versus dehydrocarbon atom separation (DAS) for **15**–**20** (DDP = didehydropyridinium cation) calculated at the RHF–UCCSD(T)/cc–pVTZ//B3LYP/cc–pVTZ level of theory.

Finally, the mechanism of abstraction of two hydrogen atoms from cyclohexane by the biradicals discussed above should be considered. We have assumed that these reactions occur by a radical mechanism. Some evidence in support of this hypothesis is obtained by considering the data in Table 1. If the two hydrogen atom abstractions involve an ionic mechanism (i.e., hydride abstraction followed by proton abstraction) rather than a radical mechanism, the most electrophilic biradicals (i.e., those with the greatest $EA_{2.30}$) should show enhanced reactivity (reaction efficiencies). This was found not to be the case. For example, biradical **10** reacts with cyclohexane more slowly than biradicals **11**–**14** even though it has the greatest $EA_{2.30}$ in this group (Table 1). Finally, the mechanism of abstraction of two hydrogen atoms from cyclohexane by the biradicals discussed above should be considered. We have assumed that these reactions occur by a radical mechanism. Some evidence in support of this hypothesis is obtained by considering the data in Table 1. If the two hydrogen atom abstractions involve an ionic mechanism (i.e., hydride abstraction followed by proton abstraction) rather than a radical mechanism, the most electrophilic biradicals (i.e., those with the greatest $EA_{2.30}$) should show enhanced reactivity (reaction efficiencies). This was found not to be the case. For example, biradical **10** reacts with cyclohexane more slowly than biradicals **11**–**14** even though it has the greatest $EA_{2.30}$ in this group (Table 1).

Theoretical disquisition

If $\Delta E_{S\text{-}T}$, $\Delta E_{2.30}$ and $EA_{2.30}$ are the main factors controlling the reactivity of *meta*–benzyne analogs in hydrogen atom abstraction reactions with cyclohexane, is it possible to determine how the barrier for hydrogen atom abstraction depends on all three factors simultaneously? The energy required to distort the DAS of a *meta*–benzyne from the minimum energy geometry to the geometry of the transition state (i.e., DAS: 2.30 Å, see above) increases the overall barrier height by some energy increment. In addition, as the DAS of the *meta*–benzyne distorts to the transition state geometry, the S–T splitting is reduced by an amount equal to $\Delta E_{2.30}$ (the energy of the triplet state is unaffected because we are considering a distortion of the singlet (ground) state only). Thus, at the transition state geometry, the S–T splitting is reduced, but it is still nonzero since the two unpaired electrons are still coupled to some extent even at a DAS of 2.30 Å. Because the two unpaired electrons must further uncouple in the transition state for hydrogen atom abstraction, some portion of the energy associated with the S–T splitting at 2.30 Å also must increase the overall barrier height. Finally, a greater $EA_{2.30}$ would be expected to decrease the overall barrier height.

Taking into account these various energy contributions, and examining their relationships to the calculated (MPW1K/6–31+G(d,p)//MPW1K/6–31+G(d,p)) activation enthalpies for hydrogen atom abstraction from methane (Table 2), the following equation was identified from a best fit of the data using *Solver* in *Microsoft Excel*,[127]

$$\Delta H^{\ddagger}_{act} = \Delta E_{2.30} - x(EA_{2.30} \times 23.06) + y(\Delta E_{S\text{-}T}+\Delta E_{2.30}) \qquad (1)$$

where $x = 0.04090$ and $y = -0.6154$. Thus, based on eq 1, the barrier height (i.e., activation enthalpy) increases by an energy increment equal to $\Delta E_{2.30}$, decreases by an energy increment equal to the coefficient x multiplied by $EA_{2.30}$ (multiplied by 23.06 to convert eV to kcal mol^{-1}) and increases by an energy increment equal to the coefficient y multiplied by the S–T splitting at 2.30 Å (i.e., $(\Delta E_{S\text{-}T}+\Delta E_{2.30})$). Note that the coefficient y indicates the percentage (ca. 62%) of the energy associated with the S–T splitting at 2.30 Å that is necessary to uncouple the unpaired electrons in the transition state. A plot of the calculated (MPW1K) activation enthalpies for the seventeen biradicals, **4**–**20**, versus the calculated activation enthalpies using eq 1 is shown in Fig. 9. Note that the slope and y–intercept for the best fit line are nearly equal to one and zero, respectively.

By using the values for $\Delta E_{S\text{-}T}$, $\Delta E_{2.30}$ and $EA_{2.30}$ (Table 1), and the calculated activation enthalpies from eq 1 (Table 2), it is now possible to "dissect" and evaluate each of the various energy contributions to the barrier heights for hydrogen atom abstraction by biradicals **4**–**20**. These contributions are shown in Table 3. As expected, $EA_{2.30}$ lowers the barrier height in all cases, the extent to which depending on its magnitude. More importantly, for the majority of the biradicals studied, the reactivity controlling factor that has the greatest influence on (increasing) the barrier height is the S–T splitting at 2.30 Å (i.e., $\Delta E_{S\text{-}T}+\Delta E_{2.30}$), although in one case (biradical **16**), it is $\Delta E_{2.30}$ that has the greatest influence on (increasing) the barrier height.

Table 2. Calculated Activation Enthalpies[a] (kcal mol^{-1}) for Hydrogen Atom Abstraction from Methane by Biradicals **4**–**20**.

	$\Delta H^{\ddagger}_{act}$ (MPW1K)	$\Delta H^{\ddagger}_{act}$ (eq 1)		$\Delta H^{\ddagger}_{act}$ (MPW1K)	$\Delta H^{\ddagger}_{act}$ (eq 1)
4	6.7	8.9	**13**	5.9	6.1
5	8.6	12.5	**14**	5.1	5.5
6	12.8	14.6	**15**	13.4	11.2
7	20.0	19.2	**16**	21.5	21.4
8	14.3	16.6	**17**	14.7	16.3
9	9.8	9.8	**18**	10.6	10.6
10	10.7	10.8	**19**	9.8	8.1
11	5.7	6.6	**20**	14.3	12.1
12	8.4	8.4			

[a] "Activation enthalpy" is the difference in enthalpy between the separated reactants and the transition state.

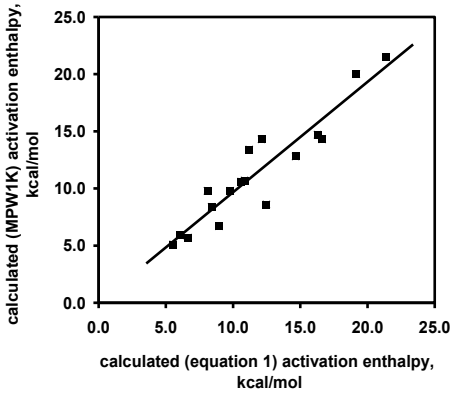

Fig. 9 Calculated (MPW1K) activation enthalpies versus calculated (equation 1) activation enthalpies for hydrogen atom abstraction from methane (as a model for cyclohexane) by biradicals **4**–**20**. The data are fit to a linear trend line ($y = 0.9653x + 0.0205$; $R^2 = 0.8799$).

Table 3. Calculated[a] Energy Contributions[b] (kcal mol^{-1}) to the Activation Enthalpies for Hydrogen Atom Abstraction from Methane by Biradicals **4**–**20**.

	structural distortion to 2.30 Å ($\Delta E_{2.30}$)	electron affinity at 2.30 Å ($EA_{2.30}$)	uncoupling of unpaired electrons at 2.30 Å ($\Delta E_{S\text{-}T}+\Delta E_{2.30}$)
4	5.1	–6.6	10.5
5	6.4	–6.4	12.6
6	9.8	–6.3	11.2
7	11.9	–5.6	12.9
8	9.7	–6.1	13.0
9	6.5	–6.0	9.5
10	8.5	–6.6	8.9
11	4.6	–6.3	8.4
12	6.1	–6.2	8.6
13	2.8	–5.6	8.0
14	2.8	–6.1	8.0
15	6.2	–6.2	11.2
16	14.7	–6.3	13.4
17	9.7	–6.6	13.4
18	5.7	–6.8	12.0
19	5.8	–6.4	8.9
20	8.8	–6.8	10.7

[a] Using equation 1 (see text). [b] Positive values increase the barrier height; negative values decrease the barrier height.

Conclusion

Perturbation of the structure of *meta*–benzyne analogs by changing the position and type of a substituent is demonstrated to influence their reactivity and to be able to convert their reactivity from less radical–like to more radical–like. Quantum chemical calculations show that the key reactivity controlling parameters are: (1) the energy required to distort the dehydrocarbon atom separation for the minimum energy geometry to the geometry of the transition state (i.e., DAS: 2.30 Å), (2) the S–T splitting at the geometry of the transition state, and (3) the electron affinity at the geometry of the transition state. By varying the substituents attached to a *meta*–benzyne analog, these three main reactivity controlling parameters can be changed such that the hydrogen atom abstraction efficiencies with cyclohexane can be "tuned" from 0% to about 20%. For polar hydrogen atom donors (such as methanol), additional reactivity controlling factors (such as hydrogen bonding) would likely need to be considered.

Acknowledgements

The authors thank the National Science Foundation for financial support of this work.

Notes and references

[a] Department of Chemistry, Purdue University
560 Oval Drive, West Lafayette, IN 47907-2084, USA
Fax: (+1)-765-494-0359
E-mail: hilkka@purdue.edu
jnash@purdue.edu
[b] Department of Chemistry
Chemical Theory Center and Supercomputing Institute, University of Minnesota, 207 Pleasant St. SE, Minneapolis, MN 55455, USA

† Electronic Supplementary Information (ESI) available: [details of any supplementary information available should be included here]. See DOI: 10.1039/b000000x/

1. W. Sander, *Accounts Chem. Res.*, 1999, **32**, 669-676.
2. H. H. Wenk, M. Winkler and W. Sander, *Angew. Chem. Int. Edit.*, 2003, **42**, 502-528.
3. K. C. Nicolaou and W. M. Dai, *Angew. Chem. Int. Edit.*, 1991, **30**, 1387-1416.
4. K. C. Nicolaou and A. L. Smith, *Accounts Chem. Res.*, 1992, **25**, 497-503.
5. J. S. Thorson, E. L. Sievers, J. Ahlert, E. Shepard, R. E. Whitwam, K. C. Onwueme and M. Ruppen, *Curr. Pharm. Design*, 2000, **6**, 1841-1879.
6. L. K. Madden, L. V. Moskaleva, S. Kristyan and M. C. Lin, *J. Phys. Chem. A*, 1997, **101**, 6790-6797.
7. L. V. Moskaleva, L. K. Madden and M. C. Lin, *Phys. Chem. Chem. Phys.*, 1999, **1**, 3967-3972.
8. H. Wang, A. Laskin, N. W. Moriarty and M. Frenklach, *P. Combust. Inst.*, 2000, **28**, 1545-1555.
9. K. Johnson, B. Sauerhammer, S. Titmuss and D. A. King, *J. Chem. Phys.*, 2001, **114**, 9539-9548.
10. S. Yamagishi, S. J. Jenkins and D. A. King, *J. Chem. Phys.*, 2002, **117**, 819-824.
11. H. Heaney, *Chem. Rev.*, 1962, **62**, 81-97.
12. G. Wittig, *Angew. Chem. Int. Edit.*, 1965, **4**, 731-737.
13. Krishnap.S, *J. Sci. Ind. Res. India*, 1970, **29**, 538-544.
14. H. Pellissier and M. Santelli, *Tetrahedron*, 2003, **59**, 701-730.
15. P. G. Wenthold and R. R. Squires, *J. Am. Chem. Soc.*, 1994, **116**, 6401-6412.
16. P. G. Wenthold, J. Hu and R. R. Squires, *J. Am. Chem. Soc.*, 1996, **118**, 11865-11871.
17. P. G. Wenthold, R. R. Squires and W. C. Lineberger, *J. Am. Chem. Soc.*, 1998, **120**, 5279-5290.
18. E. Kraka and D. Cremer, *Chem. Phys. Lett.*, 1993, **216**, 333-340.
19. A. Nicolaides and W. T. Borden, *J. Am. Chem. Soc.*, 1993, **115**, 11951-11957.
20. S. G. Wierschke, J. J. Nash and R. R. Squires, *J. Am. Chem. Soc.*, 1993, **115**, 11958-11967.
21. E. Kraka and D. Cremer, *J. Am. Chem. Soc.*, 1994, **116**, 4929-4936.
22. R. Lindh and B. J. Persson, *J. Am. Chem. Soc.*, 1994, **116**, 4963-4969.
23. R. Lindh, T. J. Lee, A. Bernhardsson, B. J. Persson and G. Karlstrom, *J. Am. Chem. Soc.*, 1995, **117**, 7186-7194.
24. R. Lindh and M. Schutz, *Chem. Phys. Lett.*, 1996, **258**, 409-415.
25. J. J. Nash and R. R. Squires, *J. Am. Chem. Soc.*, 1996, **118**, 11872-11883.
26. C. J. Cramer, J. J. Nash and R. R. Squires, *Chem. Phys. Lett.*, 1997, **277**, 311-320.
27. E. Kraka, D. Cremer, G. Bucher, H. Wandel and W. Sander, *Chem. Phys. Lett.*, 1997, **268**, 313-320.
28. R. Lindh, A. Bernhardsson and M. Schutz, *J. Phys. Chem. A*, 1999, **103**, 9913-9920.
29. K. K. Thoen and H. I. Kenttämaa, *J. Am. Chem. Soc.*, 1997, **119**, 3832-3833.
30. K. K. Thoen and H. I. Kenttämaa, *J. Am. Chem. Soc.*, 1999, **121**, 800-805.
31. E. D. Nelson, A. Artau, J. M. Price and H. I. Kenttämaa, *J. Am. Chem. Soc.*, 2000, **122**, 8781-8782.
32. E. D. Nelson, A. Artau, J. M. Price, S. E. Tichy, L. H. Jing and H. I. Kenttämaa, *J. Phys. Chem. A*, 2001, **105**, 10155-10168.
33. E. D. Nelson and H. I. Kenttämaa, *J. Am. Soc. Mass. Spectrom.*, 2001, **12**, 258-267.

34. J. M. Price and H. I. Kenttamaa, *J. Phys. Chem. A*, 2003, **107**, 8985-8995.
35. J. M. Price, K. E. Nizzi, J. L. Campbell, H. I. Kenttamaa, M. Seierstad and C. J. Cramer, *J. Am. Chem. Soc.*, 2003, **125**, 131-140.
36. J. J. Nash, K. E. Nizzi, A. Adeuya, M. J. Yurkovich, C. J. Cramer and H. I. Kenttämaa, *J. Am. Chem. Soc.*, 2005, **127**, 5760-5761.
37. A. Adeuya, L. Yang, F. S. Amegayibor, J. J. Nash and H. I. Kenttamaa, *J. Am. Soc. Mass Spectrom.*, 2006, **17**, 1325-1334.
38. L. Yang, J. J. Nash, M. J. Yurkovich, Z. Jin, N. R. Vinueza and H. I. Kenttamaa, *Org. Lett.*, 2008, **10**, 1889-1892.
39. W. Sander, R. Marquardt, G. Bucher and H. Wandel, *Pure Appl. Chem.*, 1996, **68**, 353-356.
40. W. Sander, G. Bucher, H. Wandel, E. Kraka, D. Cremer and W. S. Sheldrick, *J. Am. Chem. Soc.*, 1997, **119**, 10660-10672.
41. W. Langenaeker, F. De Proft and P. Geerlings, *J. Phys. Chem. A*, 1998, **102**, 5944-5950.
42. R. Marquardt, A. Balster, W. Sander, E. Kraka, D. Cremer and J. G. Radziszewski, *Angew. Chem. Int. Edit.*, 1998, **37**, 955-958.
43. C. J. Cramer, *J. Chem. Soc., Perkin Trans. 2*, 1999, 2273-2283.
44. G. E. Davico, R. L. Schwartz, T. M. Ramond and W. C. Lineberger, *J. Am. Chem. Soc.*, 1999, **121**, 6047-6054.
45. W. Sander and M. Exner, *J. Chem. Soc., Perkin Trans. 2*, 1999, 2285-2290.
46. E. Kraka and D. Cremer, *J. Am. Chem. Soc.*, 2000, **122**, 8245-8264.
47. W. T. G. Johnson and C. J. Cramer, *J. Am. Chem. Soc.*, 2001, **123**, 923-928.
48. H. H. Wenk and W. Sander, *Chem.-Eur. J.*, 2001, **7**, 1837-1844.
49. H. H. Wenk, A. Balster, W. Sander, D. A. Hrovat and W. T. Borden, *Angew. Chem. Int. Edit.*, 2001, **40**, 2295-2298.
50. H. H. Nam, G. E. Leroi and J. F. Harrison, *J. Phys. Chem.*, 1991, **95**, 6514-6519.
51. C. J. Cramer, *J. Am. Chem. Soc.*, 1998, **120**, 6261-6269.
52. C. J. Cramer and S. Debbert, *Chem. Phys. Lett.*, 1998, **287**, 320-326.
53. S. L. Debbert and C. J. Cramer, *Int. J. Mass Spectrom.*, 2000, **201**, 1-15.
54. Kauffman.T and Wirthwei.R, *Angew. Chem. Int. Edit.*, 1971, **10**, 20-33.
55. M. A. Bennett and H. P. Schwemlein, *Angew. Chem. Int. Edit.*, 1989, **28**, 1296-1320.
56. G. Wittig, *Naturwissenschaften*, 1942, **30**, 696-703.
57. J. D. Roberts, H. E. Simmons, L. A. Carlsmith and C. W. Vaughan, *J. Am. Chem. Soc.*, 1953, **75**, 3290-3291.
58. E. Dreher and R. Otto, *Leibigs Ann. Chem.*, 1870, **154**, 93-130.
59. O. L. Chapman, K. Mattes, C. L. Mcintosh, J. Pacansky, G. V. Calder and G. Orr, *J. Am. Chem. Soc.*, 1973, **95**, 6134-6135.
60. O. L. Chapman, C. C. Chang, J. Kolc, N. R. Rosenquist and H. Tomioka, *J. Am. Chem. Soc.*, 1975, **97**, 6586-6588.
61. I. R. Dunkin and J. G. Macdonald, *J. Chem. Soc., Chem. Comm.*, 1979, 772-773.
62. H. H. Nam and G. E. Leroi, *J. Mol. Struct.*, 1987, **157**, 301-304.
63. C. Wentrup, R. Blanch, H. Briehl and G. Gross, *J. Am. Chem. Soc.*, 1988, **110**, 1874-1880.
64. J. G. Radziszewski, B. A. Hess and R. Zahradnik, *J. Am. Chem. Soc.*, 1992, **114**, 52-57.
65. R. Warmuth, *Angew. Chem. Int. Edit.*, 1997, **36**, 1347-1350.
66. P. D. Godfrey, *Aust. J. Chem.*, 2010, **63**, 1061-1065.
67. R. R. Jones and R. G. Bergman, *J. Am. Chem. Soc.*, 1972, **94**, 660-661.
68. H. I. Kenttämaa, *Org. Mass Spectrom.*, 1994, **29**, 1-10.
69. S. J. Danishefsky and M. D. Shair, *J. Org. Chem.*, 1996, **61**, 16-44.
70. N. M. Donahue, J. S. Clarke and J. G. Anderson, *J. Phys. Chem. A*, 1998, **102**, 3923-3933.
71. W. K. Pogozelski and T. D. Tullius, *Chem. Rev.*, 1998, **98**, 1089-1107.
72. R. G. Bergman, *Accounts Chem. Res.*, 1973, **6**, 25-31.
73. A. G. Myers, S. B. Cohen and B. M. Kwon, *J. Am. Chem. Soc.*, 1994, **116**, 1255-1271.
74. P. R. Schreiner, *J. Am. Chem. Soc.*, 1998, **120**, 4184-4190.
75. S. Koseki, Y. Fujimura and M. Hirama, *J. Phys. Chem. A*, 1999, **103**, 7672-7675.
76. G. B. Jones and P. M. Warner, *J. Am. Chem. Soc.*, 2001, **123**, 2134-2145.
77. A. Baroudi, J. Mauldin and I. V. Alabugin, *J. Am. Chem. Soc.*, 2010, **132**, 967-979.
78. R. M. Batchelder, W. R. Wilson, M. P. Hay and W. A. Denny, *Br. J. Cancer Suppl.*, 1996, **27**, S52-56.
79. C. F. Logan and P. Chen, *J. Am. Chem. Soc.*, 1996, **118**, 2113-2114.
80. J. Hoffner, M. J. Schottelius, D. Feichtinger and P. Chen, *J. Am. Chem. Soc.*, 1998, **120**, 376-385.
81. P. Chen, *Angew. Chem. Int. Edit.*, 1996, **35**, 1478-1480.
82. W. N. Washburn, *J. Am. Chem. Soc.*, 1975, **97**, 1615-1616.
83. I. P. Fisher and F. P. Lossing, *J. Am. Chem. Soc.*, 1963, **85**, 1018-1019.
84. R. S. Berry, J. Clardy and M. E. Schafer, *Tetrahedron Lett.*, 1965, 1011-1017.
85. R. Marquardt, W. Sander and E. Kraka, *Angew. Chem. Int. Edit.*, 1996, **35**, 746-748.
86. W. Sander, M. Exner, M. Winkler, A. Balster, A. Hjerpe, E. Kraka and D. Cremer, *J. Am. Chem. Soc.*, 2002, **124**, 13072-13079.
87. G. Bucher, W. Sander, E. Kraka and D. Cremer, *Angew. Chem. Int. Edit.*, 1992, **31**, 1230-1233.
88. H. H. Wenk and W. Sander, *Eur. J. Org. Chem.*, 2002, 3927-3935.
89. H. Y. Wei, D. A. Hrovat, Y. R. Mo, R. Hoffmann and W. T. Borden, *J. Phys. Chem. A*, 2009, **113**, 10351-10358.
90. W. N. Washburn and R. Zahler, *J. Am. Chem. Soc.*, 1976, **98**, 7827-7828.
91. W. E. Billups, J. D. Buynak and D. Butler, *J. Org. Chem.*, 1979, **44**, 4218-4219.
92. F. Gavina, S. V. Luis, V. S. Safont, P. Ferrer and A. M. Costero, *Tetrahedron Lett.*, 1986, **27**, 4779-4782.
93. L. H. Jing, J. J. Nash and H. I. Kenttämaa, *J. Am. Chem. Soc.*, 2008, **130**, 17697-17709.
94. W. T. G. Johnson and C. J. Cramer, *J. Phys. Org. Chem.*, 2001, **14**, 597-603.

95. B. J. Jankiewicz, J. N. Reece, N. R. Vinueza, J. J. Nash and H. I. Kenttämaa, *Angew. Chem. Int. Edit.*, 2008, **47**, 9860-9865.
96. E. Buncel, D. R. Ferguson and T. G. Flynn, *Bioorg. Chem.*, 1982, **11**, 43-54.
97. A. J. Kay, A. D. Woolhouse, G. J. Gainsford, T. G. Haskell, C. P. Wyss, S. M. Giffin, I. T. McKinnie and T. H. Barnes, *J. Mater. Chem.*, 2001, **11**, 2271-2281.
98. Y. Zhang, O. A. Pavlova, S. I. Chefer, A. W. Hall, V. Kurian, L. L. Brown, A. S. Kimes, A. G. Mukhin and A. G. Horti, *J. Med. Chem.*, 2004, **47**, 2453-2465.
99. T. Cailly, F. Fabis, S. Lemaitre, A. Bouillon and S. Rault, *Tetrahedron Lett.*, 2005, **46**, 135-137.
100. S. Singh, G. Das, O. V. Singh and H. S. Han, *Tetrahedron Lett.*, 2007, **48**, 1983-1986.
101. J. W. Gauthier, T. R. Trautman and D. B. Jacobson, *Anal. Chim. Acta.*, 1991, **246**, 211-225.
102. T. Su and W. J. Chesnavich, *J. Chem. Phys.*, 1982, **76**, 5183-5185.
103. T. H. Dunning, *J. Chem. Phys.*, 1989, **90**, 1007-1023.
104. A. D. Becke, *Phys. Rev. A*, 1988, **38**, 3098-3100.
105. C. T. Lee, W. T. Yang and R. G. Parr, *Phys. Rev. B*, 1988, **37**, 785-789.
106. J. Gräfenstein, E. Kraka and D. Cremer, *Chem. Phys. Lett.*, 1998, **288**, 593-602.
107. J. Gräfenstein, A. M. Hjerpe, E. Kraka and D. Cremer, *J. Phys. Chem. A*, 2000, **104**, 1748-1761.
108. T. D. Crawford, E. Kraka, J. F. Stanton and D. Cremer, *J. Chem. Phys.*, 2001, **114**, 10638-10650.
109. V. Polo, E. Kraka and D. Cremer, *Theor. Chem. Acc.*, 2002, **107**, 291-303.
110. W. Sander, H. Wandel, G. Bucher, J. Gräfenstein, E. Kraka and D. Cremer, *J. Am. Chem. Soc.*, 1998, **120**, 8480-8485.
111. C. J. Cramer and R. R. Squires, *Org. Lett.*, 1999, **1**, 215-218.
112. E. Kraka, J. Anglada, A. Hjerpe, M. Filatov and D. Cremer, *Chem. Phys. Lett.*, 2001, **348**, 115-125.
113. B. J. Lynch, P. L. Fast, M. Harris and D. G. Truhlar, *J. Phys. Chem. A*, 2000, **104**, 4811-4815.
114. B. J. Lynch and D. G. Truhlar, *J. Phys. Chem. A*, 2001, **105**, 2936-2941.
115. W. J. Hehre, Ditchfie.R and J. A. Pople, *J. Chem. Phys.*, 1972, **56**, 2257-2261.
116. Harihara.Pc and J. A. Pople, *Theor. Chim. Acta.*, 1973, **28**, 213-222.
117. M. M. Francl, W. J. Pietro, W. J. Hehre, J. S. Binkley, M. S. Gordon, D. J. Defrees and J. A. Pople, *J. Chem. Phys.*, 1982, **77**, 3654-3665.
118. T. Clark, J. Chandrasekhar, G. W. Spitznagel and P. V. Schleyer, *J. Comput. Chem.*, 1983, **4**, 294-301.
119. M. J. Frisch, J. A. Pople and J. S. Binkley, *J. Chem. Phys.*, 1984, **80**, 3265-3269.
120. M. Winkler and W. Sander, *J. Phys. Chem. A*, 2001, **105**, 10422-10432.
121. Note that, for these calculations, we are computing the vertical electron affinity of the radical site, not the vertical electron affinity of the molecule.
122. Because the biradicals studied here contain a formal positive charge on the nitrogen atom, the states that are produced when an electron is added to the nonbonding orbital of a biradical are formally zwitterionic, i.e., they contain localized positive (π) and negative (σ) charges.
123. Frisch, M. J. et al. Gaussian 03, revision D.01, Gaussian, Inc., Pittsburgh, PA, 2003.
124. MOLPRO, version 2008.1, a package of ab initio programs, Werner, H.J., et al.
125. J. Fossey, D. Lefort and J. Sorba, *Free radicals in organic chemistry; John Wiley & Sons: New York, 1995*, 1995.
126. It is noteworthy that the dehydrocarbon atom separation (DAS) in the transition states for these systems is similar to the calculated DAS for the lowest energy triplet state of each biradical.
127. Note that Solver did not find a solution for equation 1. This equation expresses the best fit of the data.

Chemical Science RSCPublishing

ARTICLE

Table of contents

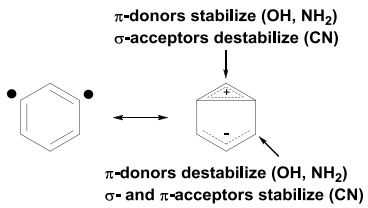

Novelty of the work: The key reactivity controlling parameters of *meta*-benzynes have been identified and demonstrated to have a major influence on their reactivity.